J Nanostruct 15(3): 1346-1353, Summer 2025

RESEARCH PAPER

Synthesis of $FeCoCrO_4$ Nanoparticles Using ginger and Malva sylvestris Extracts as Green Capping Agents: Investigation Their Magnetic Properties

Hazim Saad Jabbar Al-Maliki [1], Ahmed Ramadhan Abood [2], Raed Muslim Mhaibes [3], Huda Hadi Nameh [4], Zaid H. Mahmoud [5]*

[1] Department of Basic Sciences, College of Dentistry, University of Basrah, Basrah 61001, Iraq
[2] Department of Dentistry, College of Dentistry, Ashur university, Iraq
[3] Department of Biochemistry, College of Medicine, Misan University, Misan, Iraq
[4] College of Pharmacy, University of Hilla, Babylon, Iraq
[5] Chemistry Department, College of Sciences, University of Diyala, Iraq

ARTICLE INFO

Article History:
Received 12 April 2025
Accepted 27 June 2025
Published 01 July 2025

Keywords:
Co-precipitation
$FeCoCrO_4$ nanoparticles
Green capping agent
Magnetic properties

ABSTRACT

Ternary metal oxide ($FeCoCrO_4$) nanoparticles were synthesized using simple and straightforward co-precipitation method. Different green extracts from *ginger* and *Malva sylvestris* were used as green capping agents. The composition and phase structure of the synthesized nanoparticles were studied using X-ray diffraction pattern (XRD), confirming the formation of cubic structure. The potential of steric stabilization of the nanoparticles using the used green capping agents reflected in reduction of calculated lattice parameters, average crystallite size, and particle size. The magnetic properties of the synthesized nanoparticles were investigated using vibrating sample magnetometer (VSM), which revealed ferromagnetic behavior. The size dependence of magnetic parameters, including saturation magnetization (M_s), coercivity (H_c), remnant magnetization (M_r), anisotropy constant, and magnetic moment, was determined. The reduction in these parameters was observed for the nanoparticles synthesized in the presence of the green capping agents. The M_s for the aqueous-media-synthesized nanoparticle was 88.9 emu/g, which reduced to the 29.5 and 43.4 emu/g for those synthesized in *ginger* and *Malva sylvestris* extracts, respectively. The decrement of H_c and M_r with reducing of the particle size confirmed the decrease in magnetic domain size as the result of using the green capping agents.

How to cite this article
Al-Maliki H., Abood A., Mhaibes R., Nameh H., Mahmoud Z. Synthesis of $FeCoCrO_4$ Nanoparticles Using ginger and Malva sylvestris Extracts as Green Capping Agents: Investigation Their Magnetic Properties. J Nanostruct, 2025; 15(3):1346-1353.
DOI: 10.22052/JNS.2025.03.050

INTRODUCTION

In recent years, metal oxide nanoparticles have received considerable attention due to their unique physical and chemical properties, especially in terms of magnetic, electrical, and catalytic behavior [1-3]. Among these, mixed metal oxides stand out owing to synergistic effects arising from the combination of multiple metal components, which often result in enhanced thermal stability, improved structural integrity, and superior functional performance compared to

* Corresponding Author Email: raid.mcm@uomisan.edu.iq

single-metal oxides [4,5].

Magnetic properties of nanoparticles are of particular interest, especially as particle size is reduced to the nanoscale where the high surface-to-volume ratio and altered electronic band structures emerge. These changes have enabled the application of magnetic nanoparticles in a variety of fields including targeted drug delivery, magnetic resonance imaging (MRI), magnetic hyperthermia, and magnetic separation [6-8].

However, these properties are highly sensitive to factors such as chemical composition, particle size, synthesis method, and surface modifications [9,10]. Various synthetic routes have been employed to the preparation of mixed metal oxides, including sol-gel, auto-combustion sol-gel, co-precipitation, hydrothermal and thermal decomposition [11,12]. Of these, co-precipitation method has received tremendous attraction due to cost-effective, simple, scalability, and versatility. Recently, numerous works have been devoted to the co-precipitation of nanoparticles. For example, preparation of CdO/CuO/ZnO mixed metal oxide nanocomposite via co-precipitation method has been reported for anticancer activity application [13]. Kandasamy et al. used co-precipitation method for synthesis of ZnO/NiO/Co_3O_4 nanocomposite for solar cell application [14].

Despite its significant advantages, controlling size and stabilization of nanoparticles during synthesis by co-precipitation method remains challenging [15]. To address this, it is imperative to use of chemicals such as surfactants, polymers, and other capping agents. Due to environmental and toxicological concerns, green alternatives with lower ecological impacts are attracting considerable interest. The surface modification of nanoparticles using green capping agents has recently gained momentum due to its environmentally friendly and ability to enhance nanoparticle dispersion, reduce agglomeration, and tailor surface-related properties [16,17].

In the present work, two natural plant extracts, *ginger* and *Malva sylvestris*, were employed as capping and stabilizing agents during the synthesis process. The plant extracts contain wide variety of organic compounds, including flavonoids, terpenoids, alkaloids, and polyphenols, which have potential capability serving as steric stabilizer [18,19]. This study presents the co-precipitation synthesis of the ternary metal oxide nanoparticles, $FeCoCrO_4$ (FCCO), in the presence of different green extracts. For comparison, the FCCO was synthesized in pure aqueous medium to assess the effectiveness of the used plant extracts in stabilizing and controlling the particle size. The vibrating sample magnetometer (VSM) analysis was employed to investigate the effect of particle size on the magnetic behavior of the synthesized nanoparticles.

MATERIALS AND METHODS

Preparation of green extract

5.0 g of the *ginger* powder and *Malva sylvestris* were separately weighted and dispersed into 100 mL of deionized water and then heated at 80 °C for 1 h. After that, the mixture was isolated from the solids using paper filter. The filtrates were kept in refrigerator for following uses.

Synthesis of $FeCoCrO_4$ nanoparticles (FCCO)

The co-precipitation method was used to synthesize the FCCO nanoparticles. Different

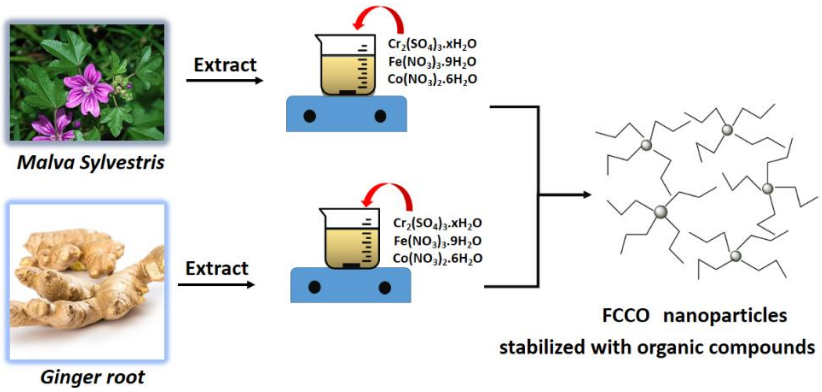

Fig. 1. Illustration for the steric hindrance caused by the green capping agents.

green capping agents were used to control the size of nanoparticles. The metal precursors were dissolved into 50 mL of the as-prepared green extract, including $Cr_2(SO_4)_3.xH_2O$ (1.0 mmol), $Fe(NO_3).9H_2O$ (1.0 mmol) and $Co(NO_3).6H_2O$ (1.0 mmol). The solution was stirred for 1 h at 50 °C. Then, pH of the solution was adjusted to 9 using addition of NaOH (0.1 M). The solution was heated at 80 °C under constant stirring to remove water by evaporation, leading to formation of the dark brown sticky gel. The gel was dried at 120 °C and then calcined at 600 °C for 6 h. The similar route was followed in pure water medium to synthesize of FCCO without addition of capping agent. Fig. 1 shows the schematic illustration of the steric stabilization of the synthesized nanoparticles using green capping agent.

Characterization

Composition and crystalline phase of the prepared nanoparticles were studied using X-ray diffraction (XRD) patterns by X'pert Pro MPD Philipls (Cu Kα, λ = 1.54 Å). Functional groups of the nanoparticles were detected using Fourier transform infrared (FTIR) spectroscopy by Bruker Tensor 27 FTIR spectrometer. Morphology of the prepared nanoparticles was studied using field emission scanning microscope (FESEM) (TESCAN BRNO-Mira3 LMU). Magnetic measurements were studied using vibrating sample magnetometer (VSM) by VSM MDKB.

RESULTS AND DISCUSSION

The XRD patterns of the synthesized nanoparticles are presented in Fig. 2, revealing the successful synthesis of cubic phase of $FeCoCrO_4$ nanoparticles. All the diffraction planes corresponded to the Bragg positions in JCPDS file no. 01-076-2496 without observing secondary phase. For a cubic structure lattice constants ($a = b = c$; $\alpha = \beta = \gamma = 90°$) can be determined as follows:

$$\frac{1}{d^2} = \frac{h^2 + k^2 + l^2}{a^2} \quad (1)$$

, where d is the lattice distance, a is the lattice constant, h, k, and l are indexes of diffraction

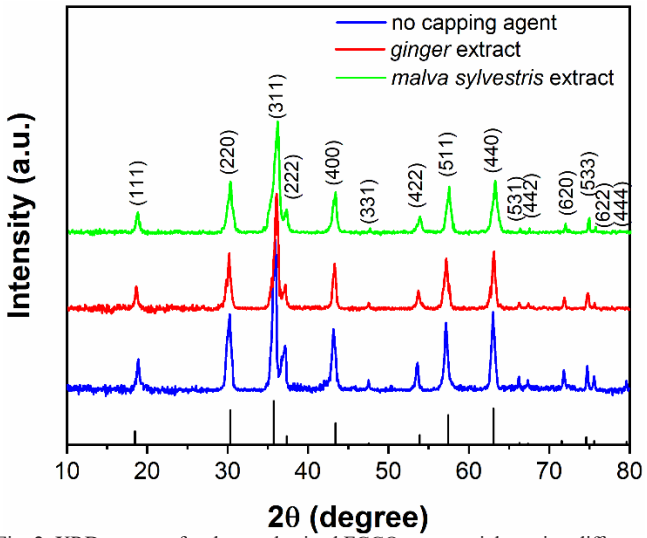

Fig. 2. XRD patterns for the synthesized FCCO nanoparticles using different capping agents.

Table 1. Calculated crystal parameters for the synthesized FCCO nanoparticles.

Synthesis condition	Lattice constant (Å)	Cell volume (Å^3)	Crystallite size (nm)
Without capping agent	8.391	590.8009	29.14
Ginger extract	8.273	566.2250	13.55
Malva Sylvestris extract	8.325	576.9693	17.67

planes. By considering the reflection of (311) at 2Θ = 35.6°, the lattice constants for the samples synthesizing in the different conditions were obtained, which are tabulated in Table1. Also, the average crystallite size for the different nanoparticles was calculated using Scherrer equation [20], reported in Table 1.

The results are in agreement with expectations, the lattice constants and crystallite sizes decreased by using of the green extract as the capping agent. The used green extracts have the significant potential serving as the efficient steric agents to limit the particle growth by hampering their accumulations.

The composition of the synthesized nanoparticles was further studied using the FTIR spectroscopy. Fig. 3a-c show the FTIR spectra of the nanoparticles before calcination at 600 °C. The existence of the functional groups corresponded to the green extracts clearly confirmed the surface modification of the nanoparticles using the capping agents. The O-H bending vibration, C-O stretching vibration, and C-H bonds are occurred at around 1600, 1400, and 2900 cm^{-1}, respectively, which are attributed to the organic compounds within the green extracts [21,22]. The sample synthesized without addition of capping agents is obviously lack of these characteristic vibration bands. After calcination of the nanoparticles, the FTIR spectra (Fig. 3d-f) exhibit the pure mixed metal oxide composition, revealing removal of the surface adsorbed organic compounds as the result of the heat treatment. The broad peaks centered 3400 cm^{-1} are related to the O-H vibrational modes due to the adsorbed water molecules [22]. The strong bands in the range 600-400 cm^{-1} are assigned to the metallic bonds, confirming the formation of the mixed metal oxides. According to the literature [23], the FCCO nanoparticles possess the spinel structure; therefore, the observed bands at around 600 and 400 cm^{-1} are reasonably attributed to the metal-oxygen vibrations at the tetrahedral (A) and octahedral (B) sites of the spinel lattice, respectively [24,25].

The FESEM images in Fig. 4 show the morphology and surface properties of the synthesized nanoparticles using the different green capping agents. In accordance with XRD results, the observed decrement in the particle sizes highlighted the capability of the used capping agents to limit crystallite aggregation by controlling the nucleation ant growth processes. As can be seen, the sample synthesized in pure water medium (Fig. 4a) exhibits the particle size in the hundreds of nanometers along with strong agglomeration, whereas the appreciable size reduction is observed for the nanoparticles synthesized by the *ginger* (Fig. 4b) and *Malva sylvestris* (Fig. 4c) extracts. The FESEM images for the samples synthesized using the green capping agent exhibit very fine nanoparticles with the sizes below 50 nm.

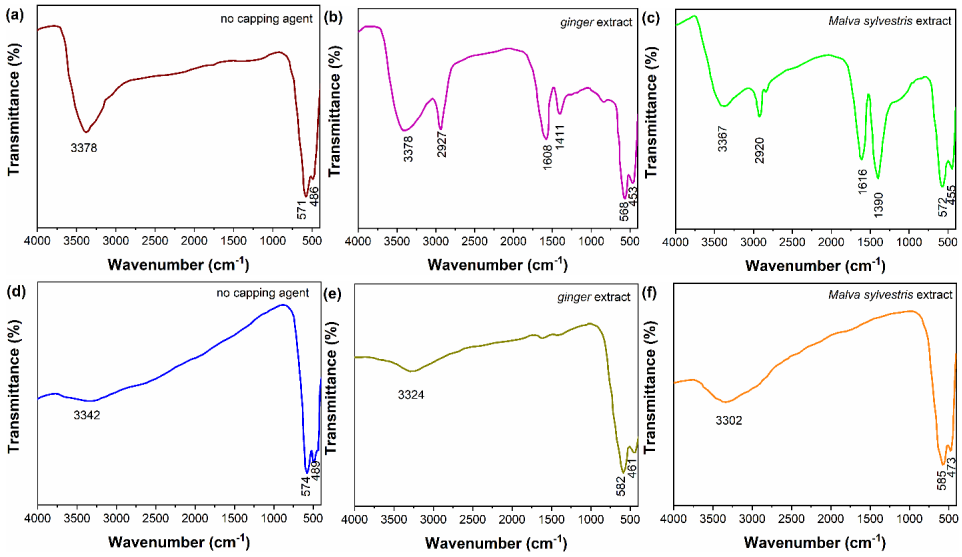

Fig. 3. FTIR spectra for the synthesized FCCO nanoparticles: before (a-c) and after calcination (d-f.).

Due to the high surface energy of the fine nanoparticles, they tend to agglomerate, leading to the formation of secondary fragments at the micrometer scale. These fragments consist of the spherical nanoparticles, which are more clearly observed at the higher magnification (Fig. 4d and 4e). Additionally, Fig. 4f-g present the particle size distribution for the FCCO nanoparticles synthesized in different conditions. As seen, the sample prepared using the *ginger* extract has the narrower size distribution. Compared to the *Malva sylvestris* extract, the organic compounds within the *ginger* extract seem to provide the greater steric hindrance, resulting in the smaller

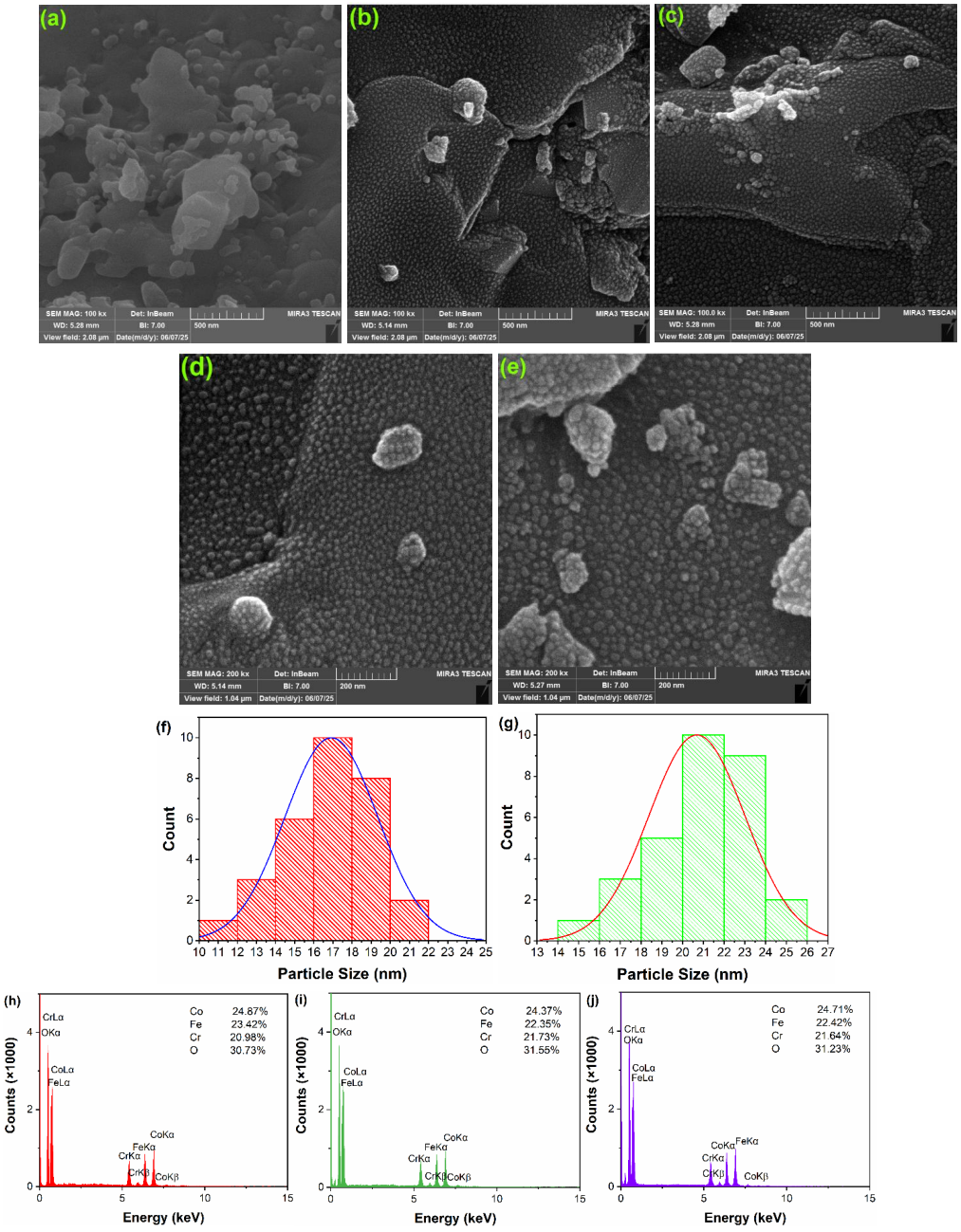

Fig. 4. FESEM images, EDX spectrum, and particle size distribution for FCCO synthesized in pure water (a, h), ginger (b, d, f, i), and Malva sylvestris extract (c, e, g, j).

FCCO nanoparticles. Moreover, the compositional analysis for the synthesized FCCO nanoparticles was performed using the EDX spectroscopy (Fig. 4h-j), confirming the existence of the constituents of the synthesized nanoparticles.

Given that the FCCO nanoparticles are composed of the Cr^{3+} (d^3), Fe^{3+} (d^5), and Co^{2+} (d^7), the magnetic behavior is primarily attributed to the magnetic moments originating from unpaired *d* electrons of these ions, which contribute to the net magnetization of the system [26,27]. The magnetic behavior of the synthesized CCFZO nanoparticles was studied using VSM analysis. Fig. 5 shows the room temperature M-H curves for the different FCCO nanoparticles, confirming the ferromagnetic properties for the nanoparticles.

According to the literature [28,29], the saturation magnetization (M_s), coercivity (H_c), and remnant magnetization (M_r) are affected by the particle size. As seen from Fig. 5, the M_s decreases with reduction in particle size, so that FCCO nanoparticles synthesized by *ginger* extract has the lowest value of M_s (29.5 emu/g). The M_s values for the FCCO nanoparticles synthesized in pure water and *Malva sylvestris* extract are 88.9 and 43.4 emu/g, respectively. Due to the enhanced surface spin disorder, decrement in the particle size lead to decrease in the saturation magnetization [30]. Moreover, the decrease in the particle size leads to the change in the term of multi-domain particle into single-domain particle, reducing the coercivity (H_c) [31]. The H_c values are 215.45, 191.51, and 211.37 Oe for the different FCCO nanoparticles, respectively synthesized in pure water, *ginger*, and *Malva sylvestris* extract. Additionally, the remnant magnetization exhibits the size-dependent behavior, where the M_r decreases with the reduction in particle size, attributed to the utilization of the green extracts. In this regard, using *ginger* extract as capping agent led to the decrease in the M_r from 7.9 to 1.8 emu/g. Moreover, the magnetic moment (n_B) was

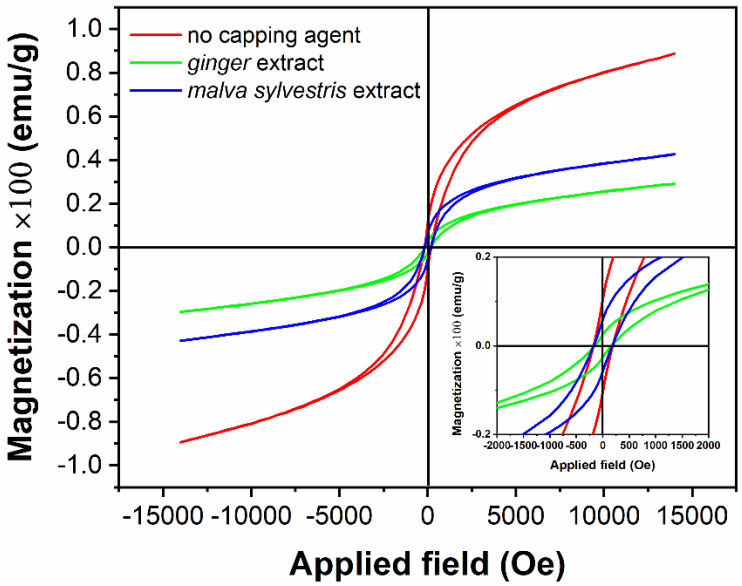

Fig. 5. Room temperature M-H curves for the synthesized FCCO nanoparticles.

Table 2. Magnetic data for the synthesized FCCO nanoparticles using different capping agents.

Magnetic parameters	no capping agent	*Ginger* extract	*Malva Sylvestris* extract
Saturation magnetization (emu/g)	88.9	29.5	43.4
Remnant magnetization (emu/g)	7.9	1.8	4.5
Coercivity (Oe)	215.45	191.51	211.37
Magnetic moment (μ_B)	3.67	1.21	1.79
Anisotropy constant (erg/g)	19951.56	5884.94	9555.68

affected by the size of the FCCO nanoparticle, as calculated by the following equation (Eq. 2) [32]:

$$n_B = \frac{M \times M_s}{5585} \quad (2)$$

where *M* is the molecular weight of the nanoparticles, M_s is the saturation magnetization, and the constant 5585 is used to convert the magnetization and molecular weight into the magnetic moment in Bohr magnetons per metal ion.

In addition, the anisotropy constant *K* was determined for the different synthesized FCCO nanoparticles. To end this, the following equation (Eq. 3) was employed [33]:

$$K = \frac{M_s \times H_c}{0.96} \quad (3)$$

As expected, the variations in both the magnetic moment and anisotropy constant were consistent with the changes in the FCCO particle size. Table 2 summarizes the magnetic measurements for the synthesized FCCO nanoparticles.

CONCLUSION

In this work, the $FeCoCrO_4$ (FCCO) nanoparticles were synthesized using the simple co-precipitation method. Different green capping agents, *ginger* and *Malva sylvestris* extracts, were used to stabilize the nanoparticles and control their sizes. The crystal structure investigations were performed for the synthesized nanoparticles, which confirmed the cubic phase for the FCCO nanoparticles. It was found that crystallite size and lattice constants changed through application of green capping agents. The FESEM images showed that the FCCO particle size decreased when *ginger* and *Malva sylvestris* extracts were used as the reaction medium for synthesizing the nanoparticles. The magnetic behavior of the FCCO nanoparticles was studied using VSM analysis, showing the size dependence of magnetic properties. The M_s for the FCCO synthesized in aqueous medium was 88.9 emu/g, whereas this value decreased to 29.5 emu/g by using of *ginger* extract. Similar trends were observed for the Hc and Mr, where FCCO synthesized in pure water and ginger extract media exhibited the coercivities of 215. 45 and 191.51 Oe and remnant magnetizations of 7.9 and 1.8 emu/g, respectively.

CONFLICT OF INTEREST

The authors declare that there is no conflict of interest regarding the publication of this manuscript.

REFERENCES

1. Rahbar M, Behpour M. Fluorite type La2Pb2O7 nanoparticles coated onto AgO as enhanced performance cathode active material for alkaline primary cell. J Power Sources. 2022;521:230887.
2. Abed SH, Shamkhi AF, Heydaryan K, Mohammadalizadeh M, Sajadi SM. Sol-gel Pechini preparation of CuEr2TiO6 nanoparticles as highly efficient photocatalyst for visible light degradation of acid red 88. Ceram Int. 2024;50(13):24096-24102.
3. Sun S, Li W, Zhang Y, Gao Q, Zhang N, Qin Y, et al. Mixed Metal Oxide Heterojunction for High-Performance Self-Powered Ultraviolet Photodetection. Small. 2024;21(4).
4. Aluko EO, Adekunle AS, Oyekunle JA, Oluwafemi OS. A Review of Nanomaterials and Microwave Synthesized Metal Oxides Nanoparticles in Schistosomiasis Diagnosis. Journal of Fluorescence. 2025.
5. Lessa TS, Santos RS, Suresh Babu R, Samyn LM, Vinodh R, de Barros ALF. Influence of sintering temperature on graphitic carbon nitride nanosheets grafted binary metal oxide for high performance asymmetric supercapacitors. Mater Lett. 2025;382:137855.
6. Kolhatkar A, Jamison A, Litvinov D, Willson R, Lee T. Tuning the Magnetic Properties of Nanoparticles. Int J Mol Sci. 2013;14(8):15977-16009.
7. Ghazi R, Ibrahim TK, Nasir JA, Gai S, Ali G, Boukhris I, et al. Iron oxide based magnetic nanoparticles for hyperthermia, MRI and drug delivery applications: a review. RSC Advances. 2025;15(15):11587-11616.
8. Shakeri-Zadeh A, Bulte JWM. Imaging-guided precision hyperthermia with magnetic nanoparticles. Nature Reviews Bioengineering. 2024;3(3):245-260.
9. Negrescu AM, Killian MS, Raghu SNV, Schmuki P, Mazare A, Cimpean A. Metal Oxide Nanoparticles: Review of Synthesis, Characterization and Biological Effects. Journal of Functional Biomaterials. 2022;13(4):274.
10. Zadehnazari A. Chemical synthesis strategies for metal oxide nanoparticles: a comprehensive review. Inorganic and Nano-Metal Chemistry. 2024;55(6):734-773.
11. Abdel-Aziz A-AB, Ghayad IM, El-Taib Heakal F, El Nashar RM. Review—Synthesis, Characterization, and Versatile Applications of Metal Oxides and Mixed Metal Oxide Nanoparticles. J Electrochem Soc. 2025;172(2):023503.
12. Ayanwale AP, Cornejo AD, González JCC, Cristóbal LFE, López SYR. Review of the Synthesis, Characterization and Application of Zirconia Mixed Metal Oxide Nanoparticles. International Journal of Research -GRANTHAALAYAH. 2018;6(8):136-145.
13. Aziz SN, Abdulwahab A, Shuga Aldeen T, Ahmed AAA. Tailoring CdO-CuO-ZnO Mixed Metal Oxide Nanocomposites for Anticancer Activity via Co-Precipitation Method. Nanotechnology, Science and Applications. 2025;Volume 18:225-244.

14. Kandasamy M, Husain A, Suresh S, Giri J, Jasim DJ, Rameshkumar P, et al. Enhanced dye-sensitized solar cell performance and electrochemical capacitive behavior of bi-functional ZnO/NiO/Co_3O_4 ternary nanocomposite prepared by chemical co-precipitation method. Journal of Science: Advanced Materials and Devices. 2024;9(2):100726.
15. Virkutyte J, Varma RS. Green synthesis of metal nanoparticles: Biodegradable polymers and enzymes in stabilization and surface functionalization. Chem Sci. 2011;2(5):837-846.
16. Doan Thi TU, Nguyen TT, Thi YD, Ta Thi KH, Phan BT, Pham KN. Green synthesis of ZnO nanoparticles using orange fruit peel extract for antibacterial activities. RSC Advances. 2020;10(40):23899-23907.
17. Peta S, Singh S. Green synthesis of zinc oxide nanoparticles using plant extract for catalysis applications. Nanoscale. 2025;17(7):3708-3713.
18. Gao J-F, Li H-Y, Pan K-L, Si C-Y. Green synthesis of nanoscale zero-valent iron using a grape seed extract as a stabilizing agent and the application for quick decolorization of azo and anthraquinone dyes. RSC Advances. 2016;6(27):22526-22537.
19. Heidari-Asil SA, Zinatloo-Ajabshir S, Alshamsi HA, Al-Nayili A, Yousif QA, Salavati-Niasari M. Magnetically recyclable ZnCo2O4/Co_3O_4 nano-photocatalyst: Green combustion preparation, characterization and its application for enhanced degradation of contaminated water under sunlight. Int J Hydrogen Energy. 2022;47(38):16852-16861.
20. Holder CF, Schaak RE. Tutorial on Powder X-ray Diffraction for Characterizing Nanoscale Materials. ACS Nano. 2019;13(7):7359-7365.
21. M. Awwad A, Albiss B. Biosynthesis Of Colloidal Copper Hydroxide Nanowires Using Pistachio Leaf Extract. Advanced Materials Letters. 2015;6(1):51-54.
22. Karpagavinayagam P, Vedhi C. Green synthesis of iron oxide nanoparticles using Avicennia marina flower extract. Vacuum. 2019;160:286-292.
23. Gupta MP, Sinha APB, Date SK. An investigation of $FeCoCrO_4$ by Mossbauer spectroscopy. Journal of Physics and Chemistry of Solids. 1978;39(12):1321-1327.
24. Patil MR, Rendale MK, Mathad SN, Pujar RB. FTIR spectra and elastic properties of Cd-substituted Ni–Zn ferrites. Int J Self-Propag High-Temp Synth. 2017;26(1):33-39.
25. To Loan NT, Hien Lan NT, Thuy Hang NT, Quang Hai N, Tu Anh DT, Thi Hau V, et al. $CoFe_2O_4$ Nanomaterials: Effect of Annealing Temperature on Characterization, Magnetic, Photocatalytic, and Photo-Fenton Properties. Processes. 2019;7(12):885.
26. Tatarchuk T. Studying the Defects in Spinel Compounds: Discovery, Formation Mechanisms, Classification, and Influence on Catalytic Properties. Nanomaterials. 2024;14(20):1640.
27. Sanchez-Lievanos KR, Stair JL, Knowles KE. Cation Distribution in Spinel Ferrite Nanocrystals: Characterization, Impact on their Physical Properties, and Opportunities for Synthetic Control. Inorganic Chemistry. 2021;60(7):4291-4305.
28. Blanco-Mantecón M, O'Grady K. Interaction and size effects in magnetic nanoparticles. J Magn Magn Mater. 2006;296(2):124-133.
29. Peddis D, Cannas C, Musinu A, Ardu A, Orrù F, Fiorani D, et al. Beyond the Effect of Particle Size: Influence of $CoFe_2O_4$ Nanoparticle Arrangements on Magnetic Properties. Chem Mater. 2013;25(10):2005-2013.
30. Li Q, Kartikowati CW, Horie S, Ogi T, Iwaki T, Okuyama K. Correlation between particle size/domain structure and magnetic properties of highly crystalline Fe3O4 nanoparticles. Sci Rep. 2017;7(1).
31. Xiang Z, Song Y, Pan D, Shen Y, Qian L, Luo Z, et al. Coercivity enhancement and magnetization process in Mn55Bi45 alloys with refined particle size. J Alloys Compd. 2018;744:432-437.
32. Singhal S, Chandra K. Cation distribution and magnetic properties in chromium-substituted nickel ferrites prepared using aerosol route. J Solid State Chem. 2007;180(1):296-300.
33. Hua Y, Zichen W, Lizhu S, Muyu Z, Jianping W, Helie L. A study on the coercivity and the magnetic anisotropy of the lithium ferrite nanocrystallite. J Phys D: Appl Phys. 1996;29(10):2574-2578.